# Synthesis and Preclinical Evaluation of 68Ga-MALAT-1 ASO for PET Imaging of MALAT-1 expressing Tumours

**Zhen-Feng Liu**
Zhejiang University School of Medicine
**Jun Yang**
Zhejiang University School of Medicine
**Qianni Ye**
Zhejiang University
**Min Yang**
Jiangsu institute of nuclear medicine
**Dong-hui Pan**
Jiangsu Institute of Nuclear Medicine
**Yu-ping Xu**
Jiangsu Institute of Nuclear Medicine
**Mengjie Dong** ( dmjlzf2016@zju.edu.cn )
Zhejiang University School of Medicine First Affiliated Hospital

**Research article**

**Keywords:** MALAT-1, antisense oligonucleotides, probe, micro PET

**Posted Date:** January 10th, 2020

**DOI:** https://doi.org/10.21203/rs.2.20606/v1

# Abstract

Background: MALAT-1 (Metastasis-Associated Lung Adenocarcinoma Transcript 1) is a large long nuclear noncoding RNA (lncRNA) that is overexpressed in an array of cancers. In this study, we designed a range of positron probes for MALAT-1 to evaluate its distribution, pharmacokinetics, and to explore whether the probe can be used for the imaging of malignant tumors with high MALAT-1 expression in vivo.

Methods: 68Ga labelling of MALAT-1 antisense oligonucleotides (68Ga–MALAT-1 ASO) was synthesized by the conjugation of MALAT-1 NOTA-ASO and 68Ga3+. Purity was assessed by radio-HPLC. Pharmacokinetic studies and cell uptake were assessed. The biodistribution and metabolism of 68Ga–MALAT-1 ASO in normal ICR and MHCC-LM3 xenograft-bearing nude mice were studied.

Results: 68Ga–MALAT-1 ASO was obtained at a radiochemical yield of 98% from a 10 min synthesis with 100 ± 50 MBq/nmol activity and > 99% purity once synthesized. The Log P was -2.53±0.19. The tracer displayed excellent stability in vitro. 68Ga–MALAT-1 ASO showed satisfactory binding ability to MHCC-LM3 cells; the biodistribution of 68Ga-MALAT-1 ASO in MHCC-LM3 tumour-bearing mice showed high levels of uptake (3.04 ± 0.11%ID/g). Micro-PET scans demonstrated the tumor specific uptake of 68Ga-MALAT-1 ASO in mouse models.

Conclusions: We conclude that 68Ga labelling of MALAT-1 ASO is a convenient approach to label tumors overexpressing MALAT-1.


# Background

MALAT-1 (Metastasis-Associated Lung Adenocarcinoma Transcript 1) is an 8.5 kb lncRNA, originally identified in non-small cell lung cancers (NSCLC) in 2003. MALAT-1 has received intense research attention [1] as it serves as an oncogenic gene during the progression of breast cancer, gastric cancer, hepatocellular carcinoma, pancreatic cancer, bladder cancer, and colorectal cancer [2, 3]. Therefore, MALAT-1 may be a diagnostic biomarker, predictive biomarker or therapeutic target for specific tumours. Gutschner et al.[4] showed that zinc-finger nucleases (ZFNs) that reduce MALAT-1 expression by 1,000-fold in lung cancer cells led to a loss of tumor growth and metastasis in mouse xenograft lung cancer models, highlighting the potential of MALAT-1 inhibitors for cancer therapeutics. Our previous studies showed that 5’ (Cy5.5) labelling of MALAT-1 ASO (antisense oligodeoxynucleotide) permits the visualization of MALAT-1 expression in carcinomas, highlighting the potential of tracking lnRNA expression with optical probes [5].

To our knowledge, lncRNA MALAT-1 ASOs have not been radiolabeled with positron nuclides and has not been investigated for PET applications. Herein, we describe the development of positron probes for lncRNA MALAT-1, to evaluate its distribution, pharmacokinetics, and tumor targeting in vivo.

# Methods

## Reagents

The 20-mer PO oligonucleotides bearing a 5-aminohexyl tether were purchased from Beijing Tsing Biotech Co., Ltd. (Beijing, China). The antisense and sense sequences used here were 5'-GGGAGTTACTTGCCAACTTG-3' and 5'-CAAGTTGGCAAGTAACTCCC-3', respectively. (HEPES), HCl (30%), acetonitrile (ACN), sodium chloride, sodium acetate, methanol, ammonium acetate, and ethanol (96%) were obtained from Merck (Darmstadt, Germany). p-SCN-Bn-NOTA) was purchased from Macrocyclics (Dallas, TX, USA). Foetal bovine serum (FBS) was obtained from Biosharp. Glen-Pak DNA purification cartridges were purchased from Glen Research. Pure water (18.2MΩ cm) was used in all reactions. Unless stated otherwise, all other chemicals used for tracer synthesis were obtained either from Acros (Geel, Belgium) or Sigma-Aldrich.

Aqueous triethylammonium acetate (TEAA) (1 M, pH 7.0) was prepared with 1 M acetic acid and 1 M TE (Sigma-Aldrich). A Thermo LCQ Deca XP plus Mass Spectrometer was used to record ESI-MS spectra. Products were isolated and purified using a HPLC C18 column (1200 series, Zorbax ODS 4.6 × 250 mm). HPLC conditions were as follows: A/B gradient; A: 2% acetonitrile in 0.1 M TEAA (pH 7.0); B: 50% acetonitrile in 0.1 M TEAA (pH 7.0); elution: 1 mL/min. A $^{68}$Ge-$^{68}$Ga generator (ITG Isotope technologies) was used to produce [$^{68}$Ga] $Cl_3$.

## Bioconjugation

Oligonucleotides were functionalized at the 5' end with hexylamine to optimize the bioconjugation and radiolabelling conditions. Figure 1 showed the conjugation of p-SCN-Bn-NOTA and MALAT-1 ASO and subsequent $^{68}$Ga complexation. MALAT-1 (100 nmol) possessing 5'-aminoalkyl linkers was dissolved in $NaHCO_3$ (15 µL of 0.1 M). Equivalents of p-SCN-Bn-NOTA (20 mg/mL) were added for 12 h at room temperature. Modified MALAT-1 ASO was then separated via the DNA purification cartridge (GlenPak) and products were purified via. HPLC. MALAT-1-ASO was ethanol-sodium acetate precipitated, HPLC purified and vacuum concentrated. NOTA-ASO samples were aliquoted, lyophilized, and frozen until use.

## $^{68}$Ga-labelling of MALAT-1 antisense oligonucleotides ($^{68}$Ga–MALAT-1 ASO)

The synthetic route is shown in Figure 1. We produced $^{68}$Ga as [$^{68}$Ga]$Cl_3$ in the $^{68}$Ge/$^{68}$Ga generator via elution with 0.05 N aq. HCl. The $^{68}Ga^{3+\ eluate}$ was mixed with the solubilized bioconjugate (5-12 nmol) that was dissolved in 1M HEPES (final pH 4.0–4.2). Reactions proceeded for 10 min at room temperature. $^{68}$Ga–MALAT-1 ASO was separated on purification cartridges and sense oligodeoxynucleotides (SO) were treated as described for ASO. Radio-HPLC was used for the confirmation of yields.

## Quality control and stability

The synthesized $^{68}$Ga-MALAT-1 ASO was assayed for purity via HPLC, pH using indicator paper and the absence of suspended precipitates by analytical HPLC.

### In Vitro Stability Analysis

In vitro stability studies of $^{68}$Ga-MALAT-1 ASO were performed in foetal bovine serum as well as in phosphate-buffered saline (PBS) solution. Briefly, 50 μL of $^{68}$Ga-MALAT-1 ASO (1 MBq) was mixed with FBS at 37°C for 30 min, 60 min, and 2h. Acetonitrile (0.5 mL) was then added to precipitate serum proteins and radio-HPLC was performed to determine serum stability. Fifty microliters of $^{68}$Ga-MALAT-1 ASO (1 MBq) was mixed with PBS (10 mM, 450 μL) for 2 h and radio-HPLC was used to confirm stability.

### Partition coefficient studies

Partition coefficients (Log *P*) of $^{68}$Ga-MALAT-1 ASO were measured through the assessment of the distribution of radioactivity in 1-octanol and phosphate buffer in a 2 mL centrifuge tube. A 10 μL of $^{68}$Ga-MALAT-1 ASO solution was added to PBS + 1-octanol (total volume: 1 mL) and centrifuged (5 min at 5000 rpm). A total of 2 samples (50 μL) taken from each layer were assayed in a γ counter. Partition coefficients (log Po/w) are shown as the log-counts in 1-octanol vs PBS layers (n=3).

### Animals

ICR female mice (body weight 18–20 g), and BALB/c nude mice (6 to 8 weeks of age) were purchased from Jiangsu Gempharmatech. The mice were raised and managed on a standard diet with free water access at our institute. All animal protocols were approved by our internal review board and followed the standard care procedures for animal use (National Research Council of USA, 1996).

### Pharmacokinetic studies

For the pharmacokinetic studies, six female ICR mice weighting 18–20 g was administrated with $^{68}$Ga-MALAT-1 ASO (7.4 MBq, 0.2 mL) by IV injection into the caudal vein. Blood samples (10 μL) were obtained from the tail at various time points from 3 min to 120 min following $^{68}$Ga-MALAT-1 ASO injection. Radioactivity was calculated as the % of dose per g of tissue per body weight (%ID/g) expressed over time. Pharmacokinetics were assayed using DAS, version 2.1.1.

### Evaluation of cellular uptake

MHCC-LM3 cells (a gift from the Key Lab, State Health Commission) were cultured in complete DMEM plus 10% FBS and 100 mg/mL pen/strep. 5'(Cy3.0)-MALAT-1 ASO was transfected into cells using Lipofectamine 2000 and confirmed by immunofluorescence [5].

MHCC-LM3 cells seeded into 6-well plates (2.5× $10^6$ cells per well) to 80% confluency were treated with $^{68}$Ga-MALAT-1 ASO (final concentration of 100 nM, 0.55 MBq $^{68}$Ga-MALAT-1 ASO) for different times (30, 60, 90,120, and 240 min). Mixtures were then washed in ice-cold PBS and centrifuged to discard the supernatants. The radioactivity in the precipitate was quantitatively measured on a γ-counter. Blocking

cellular uptake by the addition of excess PO-ASO (1 μM) was studied. These experiments were repeated four times under the same conditions.

### Biodistribution studies

Normal ICR female mice (18–20 g) were randomly divided into four groups (n=5), and the radiolabelled preparation (0.1 mL, 0.37 MBq) was IV administered into the tail vein. After 15, 30, 60, and 120 min, individual mice were sedated with $CO_2$-$O_2$ and blood, brain, heart, liver, spleen, lung, kidney, stomach, intestine, muscle, pancreas, thyroid, fat, bone, thymus, adrenal gland, and urinary bladder samples were taken and weighed. Radioactivity in each organ was assessed on a γ-counter. Values are shown as the percentage of the injected dose per gram (% ID/g) which corrected for background and decay to maintain consistency.

### Biodistribution in MHCC-LM3 xenograft-bearing nude mice

BALB/c nude mice (average weight 20±3 g, age 4-to 6-wk-old) were inoculated subcutaneously with $2.5\times10^6$ tumour cells into the right axilla. Tumor growth was monitored for 3-4 weeks until the tumors reached 0.5-1.0 $cm^3$ in volume.

Model mice were divided into four groups (n=5), which were individually injected with 3.7 MBq of $^{68}$Ga-MALAT-1 ASO via the tail vein under anaesthesia. For the non-blocked studies, mice were sacrificed and their blood, tumor and organ samples were harvested and weighed at 30, 60, and 120 min post-injection. For the blocked group of mice, we injected unlabelled MALAT-1 P-O ASO (100 nmol) followed by 0.1 Ml of $^{68}$Ga-MALAT-1 ASO (370kBq) into the tail vein after 30 min. Organ radioactivity was measured as described and expressed as % ID/g.

### In vivo micro-PET/CT imaging

Mice with MHCC-LM3 tumours were divided into group 1 (antisense group), 2 (sense group) and 3 (blocked group), (n=4 for each group). Mice were injected with 0.1 mL of $^{68}$Ga-MALAT-1 ASO (3.7 MBq) via tail vein. The images were performed at 30, 60 and 90 min after injection using a micro PET/CT scanner (Siemens Inveon MultiModality system) while the mice were maintained under isoflurane anaesthesia (1.5% isoflurane, 3% oxygen). A blocking study was performed in which 100 nmol of unlabelled MALAT-1 ASO was intravenously administered 30 min before the intravenous injection of $^{68}$Ga-MALAT-1 ASO (3.7MBq). Three-dimensional volumes of interest (VOIs) were used for the assessment of %ID/g and standard uptake value (SUV) in selected organs.

### Statistics

Quantitative data were showed as the mean ± SD, and means were compared via one-way ANOVA with SPSS V.22.0 software. P-values $\leq 0.05$ were considered significant differences.

# Results

The synthesis procedure for the NOTA-ASO conjugate is shown in Figure 1. Bioconjugation was performed via a single stage reaction of hexylamine functionalized oligonucleotides with p-SCN-Bn-NOTA. Bioconjugation efficiencies were determined by reversed phase- HPLC. We achieved only ~40% conjugation due to the limited hydrolysis of p-SCN-Bn-NOTA.

Reactions were monitored according to UV profiles at 260 nm via HPLC. Products were analysed via ESI-MS. Mass spectrometry for NOTA-ASON of the antisense sequence (5'-GGGAGTTACTTGCCAACTTG-3') yielded $[M+H]^-$ of 6779.4 (calculated, 6777.73). Mass spectrometry for NOTA-ASON of the sense sequence (5'-CTTCCCTGAAGGTTCCTCC-3') yielded $[M+H]^-$ of 6717.1 (calculated, 6716.7).

$^{68}$Ga-MALAT-1 ASO was synthesized using a single stage method from NOTA-ASO. We obtained chemical yields of 98% in 10 min using HEPES. Mild radiolabelling conditions were required for oligonucleotide radiolabelling due to the highly acidic conditions of the reaction system at high temperatures. Lower yields were observed for the sodium acetate buffer (83% after 30 min). HEPES at room temperature for thus selected for all further experiments. The specific activity of the tracer can reach 100±50 MBq/nmol. As shown in Figure 2, the radiochromatogram displayed a single radioactive and UV peak at 15 min. $^{68}$Ga-MALAT-1 ASO was successfully synthesized with radiochemical purity greater than 98%. The synthesized $^{68}$Ga-MALAT-1 ASO showed high levels of clarity and purity. The pH value was 6-7.

### *In vitro* labelling stability

For stability assessments, $^{68}$Ga-MALAT-1 ASO (3.7 MBq) was incubated in PBS (pH 7.4) or FBS for 2 h. The $^{68}$Ga-oligonucleotide remained stable in PBS at room temperature for 2 h by repeated radio-HPLC analyses, and the radiochemical purities were 99.7%, 99.5%, and 99.1% (all with radiochemical purity greater than 98%) at 30 min, 60 min and 120 min, respectively. The radiochemical purities were 99.9%, 99.6%, and 99.1% in PBS at 37°C analyses at 30 min, 60 min and 120 min, respectively.

### Lipophilicity（Log *P*）

To determine the lipophilicity of $^{68}$Ga-MALAT-1 ASO, its partition coefficient was measured in PBS (pH 7.4) and 1-octanol. The lipophilicity of $^{68}$Ga-MALAT-1 ASO (log *P* value: -2.53±0.19), suggesting poor lipid permeability.

### Cellular uptake studies

To investigate intracellular uptake, MHCC-LM3 cells were treated with 100 nM of $^{68}$Ga-MALAT-1 ASO under standard tissue culture conditions. In the non-blocked group, cellular uptake (%AD/$10^6$ cell) was 3.32±0.33, 5.65±0.91, 5.75±0.43, 5.72±0.88 and 6.30±0.85 at 30min, 60 min, 90 min, 2 h and 4 h, respectively. In contrast, cellular uptake values of 2.93±0.72 to 2.87±0.70, 3.46±0.30, 4.36±0.24 and to

4.66±0.58 were observed in the blocked group (Figure 3). Reduced levels of the cellular uptake of $^{68}$Ga-MALAT-1 ASO by MHCC-LM3 cells were observed *vs.* non-blocked cells ($P$=0.0274<0.05)

## Pharmacokinetics

The pharmacokinetic parameters obtained by the pharmacokinetic calculation program were shown in Table 1. The concentration–time curves of $^{68}$Ga–MALAT-1 ASO in mice until 120 min post-injection are shown in Figure 4. $^{68}$Ga–MALAT-1 ASO followed a 2-compartment open model: $C=1.895e^{-0.7567t} + 0.0169e^{-0.0044t}$, where C: plasma pharmacokinetic activity (% ID/g); t: time post-IV injection. The $t_{1/2}$ of distribution ($t_{1/2\alpha}$) was 10.0067 whilst the $t_{1/2}$ of elimination ($t_{1/2\beta}$) was 1261.034 min. AUC 0–t and CL were 180.685 g/L·min and 0 L/min/kg, respectively. $^{68}$Ga–MALAT-1 ASO was thus efficiently absorbed and slowly eliminated.

## Biodistribution studies

Table 2 highlights the biodistribution of $^{68}$Ga-MALAT-1 ASO which was characterized by rapid clearance from the blood, with 0.88 ± 0.14% ID/g remaining 15 min post-injection compared to 0.14 ± 0.08%ID/g after 2 h. $^{68}$Ga–MALAT-1 ASO mainly accumulated in the kidney (5 min: 8.82±1.63%ID/g, 30 min: 6.23±1.24%ID/g, 60 min: 6.27±0.89%ID/g, and 120 min, 3.30±1.02%ID/g) and liver (15 min: 4.98±1.94%ID/g, 30 min:1.86±0.55%ID/g, 60 min:1.34±0.69%ID/g, and 120 min: 0.49±0.24%ID/g), followed by the intestine and bladder, suggestive of clearance via the urinary and hepatobiliary systems (Table 2), which was also vividly confirmed through the time–activity derived from VOI analysis in the main organs (heart, liver and kidney) by micro PET scan (Table 3). The brain, lung, muscle, and bone showed a lower uptake of $^{68}$Ga-MALAT-1 ASO (Table 2).

## The biodistribution of $^{68}$Ga-MALAT-1 ASO in xenograft-bearing nude mice

To investigate the tumour uptake of $^{68}$Ga-MALAT-1 ASO in MHCC-LM3 xenograft-bearing nude mice, tumours, blood, and tissue/organs were excised for the measurement of radioactivity. The tumour distribution was 3.04 ± 0.11%ID/g at 30 min, 2.04 ± 0.04%ID/g at 60 min, and 0.40 ± 0.10%ID/g at 120 min, respectively. The tumour-to-blood (T/B) and tumour-to-muscle (T/M) ratios in the non-blocked and blocked groups were calculated for $^{68}$Ga-MALAT-1 ASO (Table 4).

## Micro PET Imaging

Table 3 shows the time–activity relationship derived from the VOI analysis in the main organs (heart, liver and kidney) in normal mice after intravenous administration by micro PET. Figure 5 shows representative PET images. $^{68}$Ga-MALAT-1 ASO was observed to bind to MHCC-LM3 tumours peaked at 30 min post-injection, then declined over time. The overall image contrast was reduced starting at 60 min.

PET analysis was used to measure blood clearance rates and the tissue specific uptake of $^{68}$Ga-MALAT-1 ASO. All Micro-PET findings were consistent with the biodistribution studies. As seen in Table 5, the

tumour/non-tumour (T/NT) ratios were shown as a function of time. The tumour/muscle ratios were 1.639, 2.397, 2.342, 1.592, 1.445, and 1.254 at 30, 60, 120, 240, 360, and 480 min, respectively.

In the blocked group, study was performed in which 100 nmol of unlabelled PO MALAT-1 ASO was intravenously administered 30 min before the intravenous injection of $^{68}$Ga-MALAT-1 ASO. The results showed that the unlabelled ASO significantly reduced $^{68}$Ga-MALAT-1 ASO tumour uptake ($p$=0.002), confirming the specificity of the labelled probe (Figure 6). No tumor uptake was observed in the sense group.

# Discussion

Since the association between MALAT-1 and NSCLC has been identified, its important roles in cancer have been considered a paradigm. The expression of MALAT-1 was found to be upregulated in numerous types of tumours, and MALAT-1 promotes tumour cell growth and metastasis [6]. MALAT-1 is upregulated in hepatocellular carcinoma where it activates Wnt signalling and SRSF1, both of which promote cancer growth [7]. Guo and colleagues [8] demonstrated that MALAT-1 regulates caspase-3, caspase-8, Bax, Bcl-2, and BclxL in cervical cancer cells to promote growth and survival. Tano and coworkers [9] showed that MALAT-1 enhances cell motility through upregulating cell motility-related genes including CTHRC1, CCT4, HMMR and ROD1 both at the transcriptional and post transcriptional level. Ying et al. [10] reported the pro-metastatic role of MALAT-1 in bladder cancer. In these cells, MALAT-1 silencing led to a loss of epithelial–mesenchymal transition (EMT).

MALAT-1 is an attractive biomarker and therapeutic target [11, 12] for a range of human cancers including nasopharyngeal carcinoma [13], breast cancer [14], NSCLC [15], epithelial ovarian cancer [17], and osteosarcoma [16]. In a relatively large clinical trial, Peng et al. [11] showed that ncRNAs of MALAT-1, miR-485-5p, miR-1254, and miR-574-5p can distinguish NSCLC from healthy tissue with high sensitivity/specificity. In terms of sampling, MALAT-1 levels in the serum represented a diagnostic marker for NSCLC metastasis. Mei et al. [18] showed that MALAT-1 can distinguish cancerous tissue from healthy tissue with an AUC of 0.85 (95% CI: 0.82–0.88) and a DOR of 13 (95% CI: 8.00–21.00) in a meta-analysis. Moreover, a sensitivity of 0.74 (95% CI: 0.64–0.82) and a specificity of 0.83 (95% CI: 0.75–0.88) showed MALAT-1 had relatively high accuracy in human cancer detection. Zhang and colleagues [13] showed that serum MALAT-1 levels can distinguish breast cancer from benign breast tumours.

MALAT-1 can be targeted therapeutically in vivo through a number of approaches, including RNAi, antisense oligonucleotides, and small molecule inhibitors [18]. Compared with siRNAs, antisense oligonucleotides provide higher silencing efficiencies due to their high levels of nuclear targeting, to which cellular lncRNAs translocate. [12]. Gutschner and colleagues [20] showed a loss of tumor growth in the lungs of MALAT-1 ASO vs. control ASO groups, concluding that MALAT-1 targeting with ASO represents a novel therapeutic approach for the prevention of lung cancer metastasis. Our previous study identified 5’ (Cy5.5)-MALAT-1 ASO, a near-infrared molecular imaging probe, showed promising approach for specific

detection of tumours over-expressed MALAT-1 in vivo. The probe can selectively bind to MHCC-LM3 cells and be absorbed by cells, and its retention is time-dependent and concentration-dependent [3].

To develop novel PET molecular imaging probes, it is necessary to consider its chemical yield and radiochemical yield. In the present study, the chemical yield using HEPES buffer reached 98% within 10 min, and $^{68}$Ga-MALAT-1 ASO was successfully synthesized with radiochemical purity greater than 98%. The $^{68}$Ga-oligonucleotide remained stable in PBS and serum, and the radiochemical purity was higher than 98% for 120 min, which meets the requirements of a molecular probe to be used for further animal exploratory research.

LogP represents a compounds lipid-water partition coefficient, which is the ratio of the concentration of a compound in equilibrium between the lipid phase and the water phase. The smaller the lipid-water partition coefficient is, the more soluble the compound is in water, whereas the conversely, less soluble it is in the lipid phase. In this study, the lipid-water partition coefficient of the $^{68}$Ga-MALAT-1 ASO radioactive probe was calculated (logP=-2.5287 ± 0.1906), suggesting that the $^{68}$Ga-MALAT-1 ASO molecular probe had strong water solubility, which inferred that the molecular probe was highly radioactive in the urinary system, mainly through excretion by the urinary system, and this conclusion was further confirmed by the study of normal animals in vivo.

In this study, a positron probe of $^{68}$Ga-MALAT-1 ASO for high expression of MALAT-1 was synthesized. We confirmed high levels of uptake of the probe into MHCC-LM3 cells over time. In blocking experiments, the cellular uptake of $^{68}$Ga-MALAT-1 ASO by MHCC-LM3 cells was reduced ($P = 0.0274 < 0.05$), indicating that $^{68}$Ga-MALAT-1 ASO selectively targeted cells overexpressing MALAT-1.

The results of the biodistribution studies disclosed that $^{68}$Ga-MALAT-1 ASO initially distributed to the liver, but then predominantly accumulated in the kidneys (~ 30 min). The signal then decreased over time. After 120 min, over 30% of the signal (3.30 ± 1.02%ID/g) remained in the kidney compared to 30 min (8.82 ± 1.63%ID/g). This demonstrated that $^{68}$Ga-MALAT-1 ASO was mainly excreted by the urinary tract and hepatobiliary system.

Micro PET images from the MHCC-LM3 cell xenograft mouse models (Fig. 5) provided further evidence for the in vivo tumor targeting of $^{68}$Ga-MALAT-1 ASO. The $^{68}$Ga-MALAT-1 ASO uptake in the tumour showed an increased tumour/muscle ratio from 30, 60, to 120 min, which were1.639, 2.097, and 2.362, respectively, and then deceased over time. The in vivo experiments in tumour-bearing mice showed that the radioactivity uptake in the tumour tissues was the highest 30 min after intravenous injection of $^{68}$Ga-MALAT-1 ASO (3.04 ± 0.11% ID/g), but the ratio of tumour/muscle (2.397 ± 0.304) after 60 min was significantly higher than the ratios at the other observation times.

For tumor probe development, high specificity is an important prerequisite. We performed competition assays to further confirm the in vivo specificity of the probe. Before injection of $^{68}$Ga-MALAT-1 ASO, the competitive inhibition test was carried out by injecting MALAT-1 ASO. The uptake of $^{68}$Ga-MALAT-1 in the

tumour tissue significantly decreased (60 min, 0.73 ± 0.00%ID/g), and the tumour/blood ratio and tumour/muscle ratio both decreased significantly (0.58 ± 0.61, 0.66 ± 0.57, respectively), suggesting that this is a target-specific probe. Similar to a previous study, the kidney signal was high in the blocking experiment, suggesting that the probe was primarily cleared from the urinary tract. Moreover, it is necessary to conduct further research on the modification of molecular structure in the future to reduce the radioactive uptake by the kidney and increase the radioactive uptake by the tumour tissue.

# Conclusions

In the present research, we present a radiolabelled $^{68}$Ga-MALAT-1 ASO to image liver cancer in the MHCC-LM3 tumour model by a facile method. The radiolabelling was completed within 10 min, and the radiochemical yield reached 98%. The biodistribution of $^{68}$Ga-MALAT-1 ASO was characterized by rapid blood clearance through the urinary system. In vivo PET imaging further confirmed that $^{68}$Ga-MALAT-1 ASO had high tumour uptake (3.04 ± 0.11%ID/g) 30 min after i.v. injection. Moreover, the pharmacokinetic parameters of $^{68}$Ga-MALAT-1 ASO were obtained and showed a fast CL. Therefore, the high accumulation of $^{68}$Ga-MALAT-1 ASO in tumours expressing MALAT-1 demonstrates that the radio compound can be used as a potential positron molecular probe.

# Abbreviations

MALAT-1: Metastasis-Associated Lung Adenocarcinoma Transcript 1; lncRNA: long nuclear noncoding RNA; ASO: antisense oligonucleotide; CL: clearance rate; T/NT: tumour/non-tumour ratios; DMEM: Dulbecco's modified Eagle medium.

# Declarations

### Ethics approval and consent to participate

Animal studies were approved by the Institutional Animal Care and Use Committee of the First Affiliated Hospital of Zhejiang University, and the National Institutes of Health Guidelines of the USA (National Research Council of USA, 1996).

### Consent for publication

Not applicable.

### Availability of data and materials

The datasets used and/or analysed during the current study are available from the corresponding author on reasonable request.

### Competing interests

The authors declare that they have no competing interests.


### Funding

This project supported by the National Natural Science Foundation of China (Grant No. 81771884); The funding body only provided financial support, and the design of the study, analysis and interpretation of data and the manuscript writing were independently completed by the authors of this paper


### Author's contributions

QNY, DHP, and YPX were responsible for the model development and collected data. MY, ZFL and MJD were responsible for the conception and design. JY were responsible for the analysis. ZFL was responsible for the first draft of the manuscript. All authors were responsible for the interpretation and important intellectual input. All authors read and approved the final manuscript.


### Acknowledgements

Not applicable



### Author details

1.Department of Nuclear Medicine, The First Affiliated Hospital, Zhejiang University School of Medicine, Hangzhou, 310003, P.R. China.

2.Molecular Imaging Centre, Jiangsu institute of nuclear medicine, Jiangsu Province, 214063, P.R. China.


## References


1. Ji P, Diederichs S, Wang W, Boing S, Metzger R, Schneider PM, et al. MALAT-1, a novel noncoding RNA, and thymosin beta4 predict metastasis and survival in early-stage non-small cell lung cancer. Oncogene. 2003 (39); 22:8031–41
2. Zhang J, Zhang B, Wang T, Wang H. LncRNA MALAT-1 overexpression is an unfavorable prognostic factor in human cancer: evidence from a meta-analysis. Int J Clin Exp Med. 2015; 8 (4):5499–505.
3. Li Z, Dou P, Liu T, He S.Application of Long Noncoding RNAs in Osteosarcoma: Biomarkers and Therapeutic Targets. Cell Physiol Biochem.2017; 42 (4):1407-1419.
4. Gutschner T, Baas M, Diederichs S. Noncoding RNA gene silencing through genomic integration of RNA destabilizing elements using zinc finger nucleases. Genome Res. 2011;21 (11):1944-54.
5. Dong MJ, Wang CQ, Wang GL, Wang YH, Liu ZF.Development of novel long noncoding RNA MALAT-1 near-infrared optical probes for in vivo tumour imaging. Oncotarget. 2017; 8(49):85804-85815.
6. Gutschner T, Hämmerle M, Diederichs S. MALAT-1-a paradigm for long noncoding RNA function in cancer. J Mol Med (Berl) 2013;91(7):791–801.

7. Malakar P, Shilo A, Mogilevsky A, et al. Long Noncoding RNA MALAT-1 Promotes Hepatocellular Carcinoma Development by SRSF1 Upregulation and mTOR Activation. Cancer Res. 2017 ;77(5):1155-1167.
8. Guo F, Li Y, Liu Y, Wang J, Li Y, Li G. Inhibition of metastasis-associated lung adenocarcinoma transcript 1 in CaSki human cervical cancer cells suppresses cell proliferation and invasion. Acta Biochimica et Biophysica Sinica (Shanghai) 2010; 42(3): 224-9.
9. Tano K, Mizuno R, Okada T, Rakwal R, Shibato J, Masuo Y, et al. MALAT-1 enhances cell motility of lung adenocarcinoma cells by influencing the expression of motility-related genes. FEBS Letters. 2010; 584(22): 4575–80.
10. Ying L, Chen Q, Wang Y, Zhou Z, Huang Y, Qiu F. Upregulated MALAT-1 contributes tobladder cancer cell migration by inducing epithelial-to-mesenchymal transition. Molecular BioSystems. 2012; 8(9): 2289–94.
11. Yarmishyn AA, Kurochkin IV. Long noncoding RNAs: a potential novel class of cancer biomarkers. Front Genet. 2015; 6:145.
12. Fatima R, Akhade VS, Pal D, Rao SM. Long noncoding RNAs in development and cancer: potential biomarkers and therapeutic targets. Mol Cell Ther. 2015; 3:5
13. He B, Zeng J, Chao W, et al. Serum long non-coding RNAs MALAT-1, AFAP1-AS1 and AL359062 as diagnostic and prognostic biomarkers for nasopharyngeal carcinoma. Oncotarget. 2017; 8: 41166–41177.
14. Zhang R, Xia Y, Wang Z, et al. Serum long non coding RNA MALAT-1 protected by exosomes is up-regulated and promotes cell proliferation and migration in non-small cell lung cancer. Biochem Biophys Res Commun. 2017; 490(2): 406–414.
15. Peng H, Wang J, Li J, et al. A circulating non-coding RNA panel as an early detection predictor of non-small cell lung cancer. Life Sci. 2016;151:235–242.
16. Huo Y, Li Q, Wang X, et al. MALAT-1 predicts poor survival in osteosarcoma patients and promotes cell metastasis through associating with EZH2. Oncotarget. 2017;8 (25):46993–47006.
17. Li ZX, Zhu QN, Zhang HB, Hu Y, Wang G, Zhu YS. MALAT-1: a potential biomarker in cancer. Cancer Manag Res. 2018 ;10:6757-6768.
18. Mei H, Liu Y, Zhou Q, Hu K, Liu Y. Long noncoding RNA MALAT-1acts as a potential biomarkerin cancer diagnosis and detection: a meta-analysis. Biomark Med. 2019;13(1):45-54.
19. Li CH, Chen Y. Targeting long non-coding RNAs in cancers: progress and prospects. Int J Biochem Cell Biol. 2013; 45(8):1895–910.
20. Gutschner T, Hämmerle M, Eissmann M, Hsu J, Kim Y, Hung G, Revenko A, Arun G, Stentrup M, Gross M, Zörnig M, MacLeod AR, Spector DL, Diederichs S. The noncoding RNA MALAT-1 is a critical regulator of the metastasis phenotype of lung cancer cells. Cancer Res. 2013; 73(3):1180–89

# Tables

Table 1. Pharmacokinetic parameters of $^{68}$Ga–MALAT-1 ASO in ICR mice

| Parameters | Value |
|---|---|
| $t_{1/2\alpha}$ (min) | 10.067 |
| $t_{1/2\beta}$ (min) | 1261.034 |
| V1 (L/kg) | 0 |
| CL (L/min/kg) | 0 |
| $K_{10}$ ($min^{-1}$) | 0.011 |
| $K_{12}$ ($min^{-1}$) | 0.044 |
| $K_{21}$ ($min^{-1}$) | 0.014 |
| $AUC_{(0-t)}$ (μg/L·min) | 180.685 |
| $AUC_{(0-\infty)}$ (μg/L·min) | 424.662 |

Table 2.Biodistribution profile of $^{68}$Ga–MALAT-1 ASO in normal ICR mice (n = 5) (,%ID/g)

| Tissue/organ | % ID/g (% injected dose per gram) | | | |
|---|---|---|---|---|
| | 15min | 30min | 60min | 120min |
| Blood | 0.88±0.14 | 0.44±0.30 | 0.18±0.06 | 0.14±0.08 |
| brain | 0.08±0.05 | 0.05±0.01 | 0.05±0.02 | 0.03±0.02 |
| Heart | 0.46±0.11 | 0.18±0.02 | 0.15±0.05 | 0.13±0.05 |
| Liver | 4.98±1.94 | 1.86±0.55 | 1.34±0.69 | 0.49±0.24 |
| Spleen | 0.49±0.13 | 0.27±0.04 | 0.28±0.08 | 0.16±0.05 |
| Lungs | 0.86±0.21 | 0.27±0.09 | 0.22±0.07 | 0.11±0.02 |
| Kidney | 8.82±1.63 | 6.23±1.24 | 6.27±0.89 | 3.30±1.02 |
| Stomach | 0.51±0.19 | 1.42±0.27 | 0.57±0.47 | 0.13±0.09 |
| Intestine | 2.28±1.07 | 0.88±0.23 | 1.62±1.52 | 0.40±0.13 |
| Muscle | 0.65±0.52 | 0.54±0.32 | 0.48±0.24 | 0.41±0.07 |
| Pancreas | 0.28±0.02 | 0.17±0.04 | 0.17±0.08 | 0.11±0.07 |
| thyroid | 1.01 ±0.22 | 1.11±0.30 | 0.73±0.16 | 1.45±1.99 |
| Fat | 0.80±0.35 | 0.54±0.29 | 0.34±0.07 | 0.25±0.12 |
| Bone | 0.70±0.29 | 0.55±0.24 | 0.82±0.32 | 0.63±0.40 |
| Thymus | 0.68±0.52 | 0.33±0.24 | 0.19±0.04 | 0.28±0.11 |
| adrenal gland | 1.47±0.37 | 1.15±0.49 | 1.02±0.32 | 1.02±0.74 |
| Bladder | 3.38±1.45 | 1.21±0.47 | 0.68±0.35 | 0.62+0.25 |

Table 3.Time–activity profile derived from the VOI analysis in the main organs (heart, liver and kidney) in normal mice after intravenous administration by micro PET (n = 5)

| TIMES (S) | ORGANS | | | | | |
|---|---|---|---|---|---|---|
| | Heart | | Liver | | Kidney | |
| | %ID/g(mean) | SD | %ID/g(mean) | SD | %ID/g(mean) | SD |
| 30 | 1.8689 | 0.2359 | 4.6481 | 0.5916 | 6.5619 | 0.268 |
| 90 | 1.4178 | 0.1783 | 7.7526 | 0.2826 | 10.365 | 0.579 |
| 150 | 1.0486 | 0.0632 | 8.2524 | 0.285 | 13.201 | 0.693 |
| 210 | 0.968 | 0.1465 | 7.5431 | 0.4055 | 13.079 | 0.609 |
| 270 | 0.8831 | 0.1837 | 7.4022 | 0.3181 | 12.161 | 0.823 |
| 375 | 0.6539 | 0.0937 | 7.2925 | 0.4253 | 11.567 | 1.15 |
| 525 | 0.6256 | 0.102 | 6.8709 | 0.0185 | 11.147 | 1.008 |
| 675 | 0.5838 | 0.0464 | 5.9855 | 0.6317 | 10.739 | 0.68 |
| 825 | 0.5789 | 0.1095 | 5.7542 | 0.6141 | 10.411 | 0.243 |
| 1050 | 0.3561 | 0.0089 | 4.2088 | 0.7047 | 10.271 | 0.133 |
| 1350 | 0.2454 | 0.0733 | 3.9126 | 0.7825 | 9.2721 | 1.123 |
| 1650 | 0.1727 | 0.0035 | 2.7761 | 0.5675 | 8.364 | 1.382 |
| 2100 | 0.1612 | 0.0118 | 2.2783 | 0.1009 | 7.6267 | 0.557 |
| 2700 | 0.1475 | 0.0146 | 1.9493 | 0.0856 | 7.3774 | 0.587 |
| 3300 | 0.1355 | 0.0058 | 1.6605 | 0.3285 | 6.7176 | 0.127 |

Table 4. The biodistribution of $^{68}$Ga-MALAT-1 ASO in xenograft-bearing nude mice（%ID/g）

| Tissue/organ | Non-block | | | Block |
|---|---|---|---|---|
| | 30min | 60min | 120min | 60min |
| Blood | 2.32±0.22 | 0.43±0.47 | 0.59±0.1 | 1.23±0.57 |
| brain | 0.14±0.04 | 0.09±0.05 | 0.03±0.01 | 0.07±0.03 |
| Heart | 0.79±0.17 | 0.48±0.26 | 0.17±0.03 | 0.37±0.09 |
| Liver | 1.33±0.24 | 0.77±0.19 | 1.64±0.17 | 1.21±0.12 |
| Spleen | 1.21±0.45 | 0.68±0.07 | 0.52±0.11 | 0.78±0.12 |
| Lungs | 1.37±0.39 | 0.44±0.07 | 0.37±0.02 | 0.65±0.13 |
| Kidney | 174.99±7.17 | 145.70±32.09 | 214.30±11.42 | 206.52±7.21 |
| Stomach | 1.43±0.79 | 0.24±0.06 | 1.39±0.31 | 1.69±0.18 |
| Intestine | 0.54±0.09 | 0.45±0.15 | 0.32±0.03 | 0.46±0.11 |
| Muscle | 0.33±0.07 | 0.28±0.15 | 0.10±0.01 | 0.63±0.21 |
| Pancreas | 0.52±0.31 | 0.37±0.14 | 0.12±0.03 | 0.47±0.25 |
| thyroid | 0.49±0.07 | 0.41±0.25 | 0.33±0.23 | 1.01±0.30 |
| Fat | 0.50±0.18 | 0.53±0.22 | 0.32±0.17 | 0.55±0.39 |
| Bone | 0.44±0.03 | 0.24±0.09 | 0.41±0.11 | 0.83±0.39 |
| Tumor | 3.04±0.11 | 2.04±0.04 | 0.40±0.10 | 0.73±0.00 |
| Tumor /Blood | 1.30±0.53 | 8.47±0.02 | 0.71±0.10 | 0.58±0.61 |
| Tumor/muscle | 6.89±3.35 | 8.1725±0.12 | 3.41±0.95 | 0.66±0.57 |

Table 5. The tumour/non-tumour (T/NT) ratio in xenograft-bearing nude mice at different times as evaluated by micro PET

| T/NT | 30min | SD | 60min | SD | 120min | SD | 240min | SD | 360min | SD | 480min | SD |
|---|---|---|---|---|---|---|---|---|---|---|---|---|
| T/Muscle | 1.639 | 0.211 | 2.397 | 0.304 | 2.342 | 0.435 | 1.592 | 0.355 | 1.445 | 0.1720 | 1.254 | 0.268 |
| T/Liver | 0.035 | 0.084 | 0.013 | 0.004 | 0.007 | 0.002 | 0.009 | 0.007 | 0.013 | 0.0039 | 0.019 | 0.019 |
| T/Brain | 3.202 | 0.481 | 4.005 | 0.576 | 2.989 | 0.346 | 2.018 | 0.095 | 3.341 | 0.415 | 5.556 | 1.490 |
| T/Bone | 1.474 | 0.296 | 1.974 | 0.493 | 1.108 | 0.849 | 1.75 | 0.047 | 3.288 | 0.756 | 0.977 | 0.483 |
| T/Kidney | 0.003 | 0.003 | 0.002 | 0.001 | 0.002 | 0.001 | 0.002 | 0.004 | 0.01 | 0.009 | 0.016 | 0.001 |

# Figures

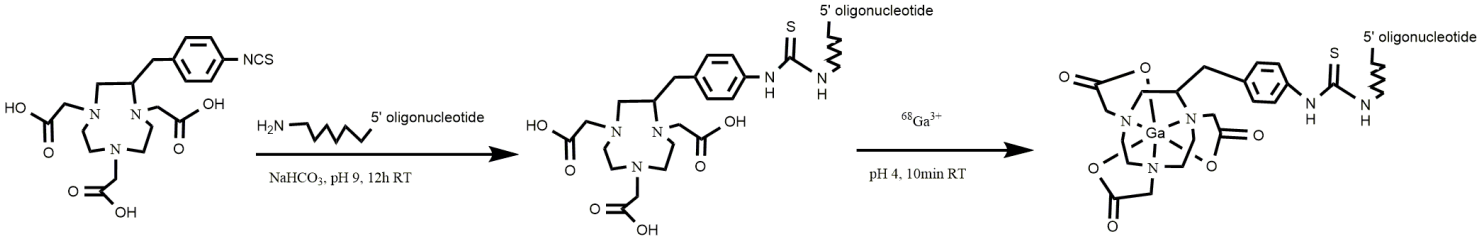


**Figure 1**

Scheme of the conjugation reaction between p-SCN-Bn-NOTA and MALAT-1 ASO and subsequent 68Ga complexation. RT = room temperature

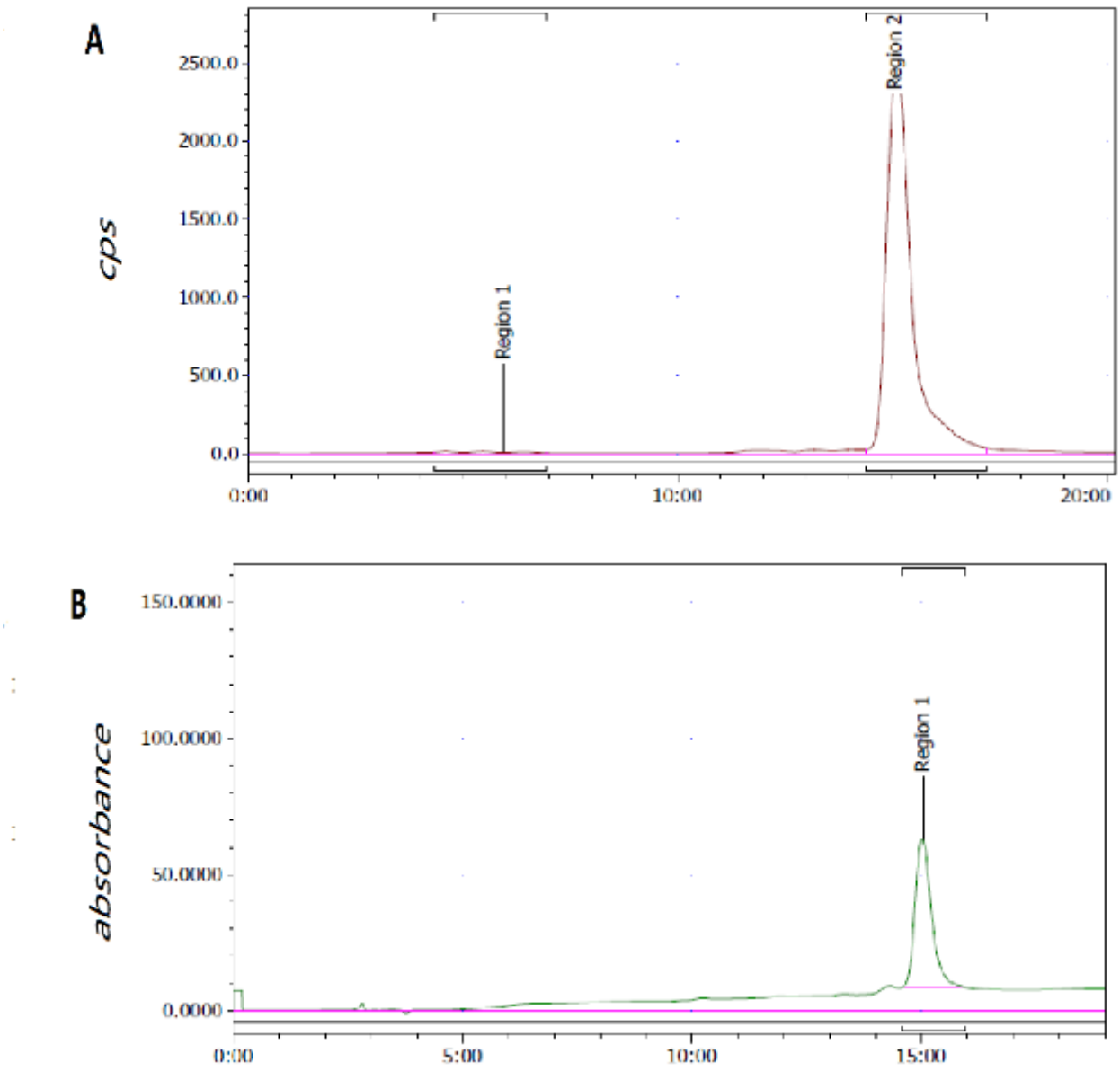


## Figure 2

Chromatograms from analytical HPLC. A: Radiochromatogram of the purified 68Ga-MALAT-1 ASO. B: UV chromatogram of 68Ga-MALAT-1 ASO.

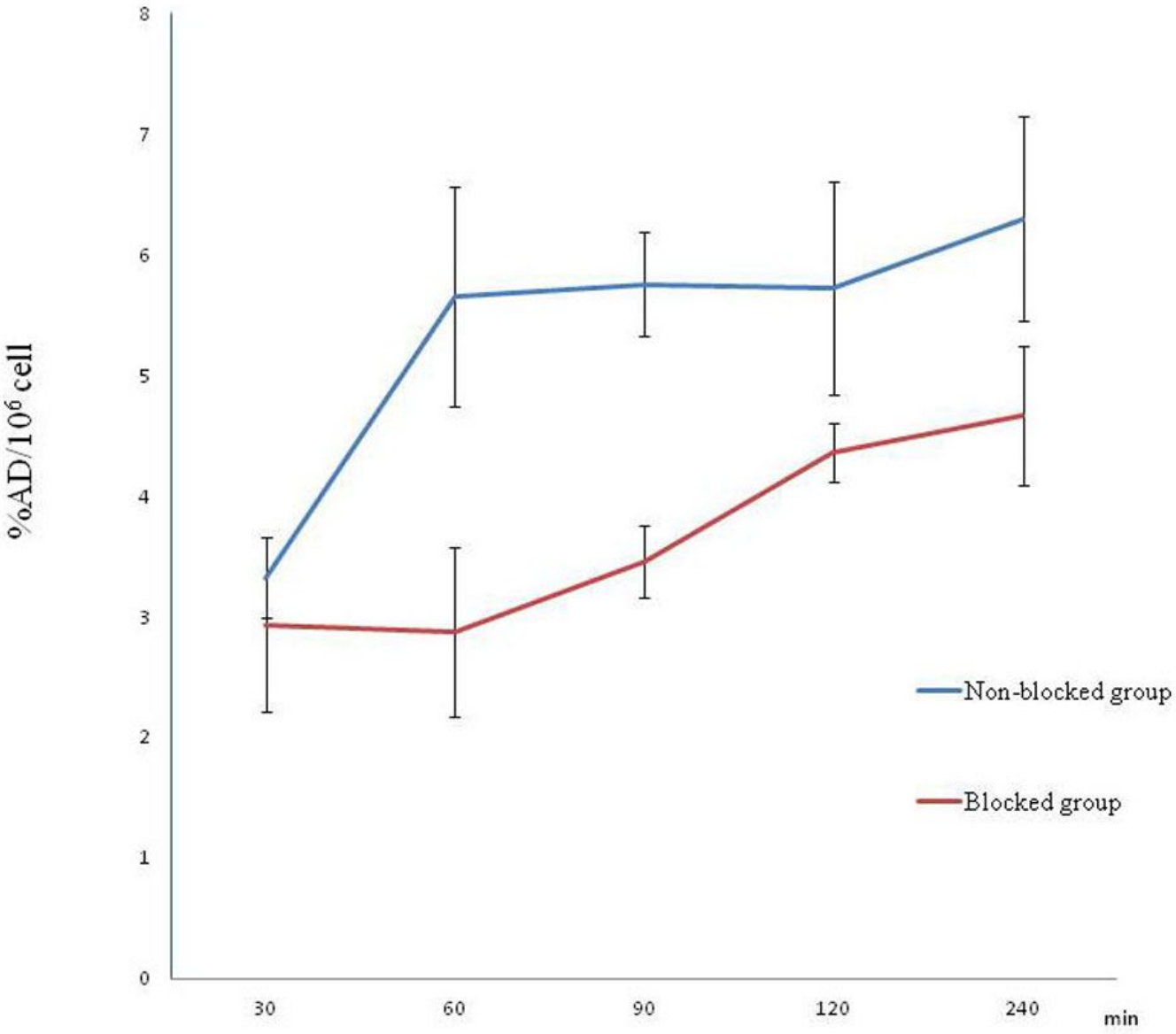


## Figure 3

MHCC-LM3 cell uptake studies in the non-blocked and blocked groups.

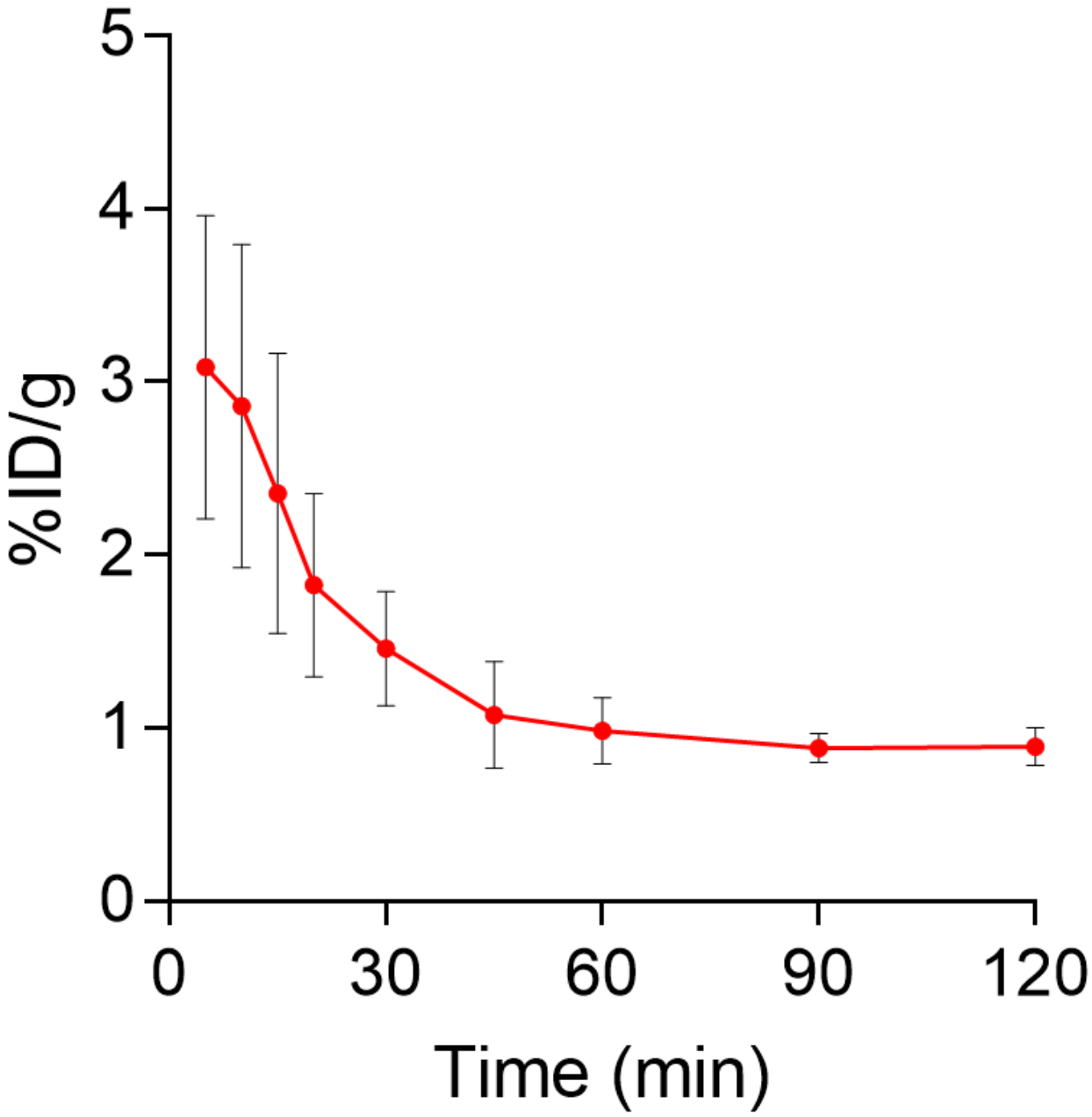


**Figure 4**

%ID/g–time curve for 68Ga–MALAT-1 ASO in ICR mice until 120 min after injection.

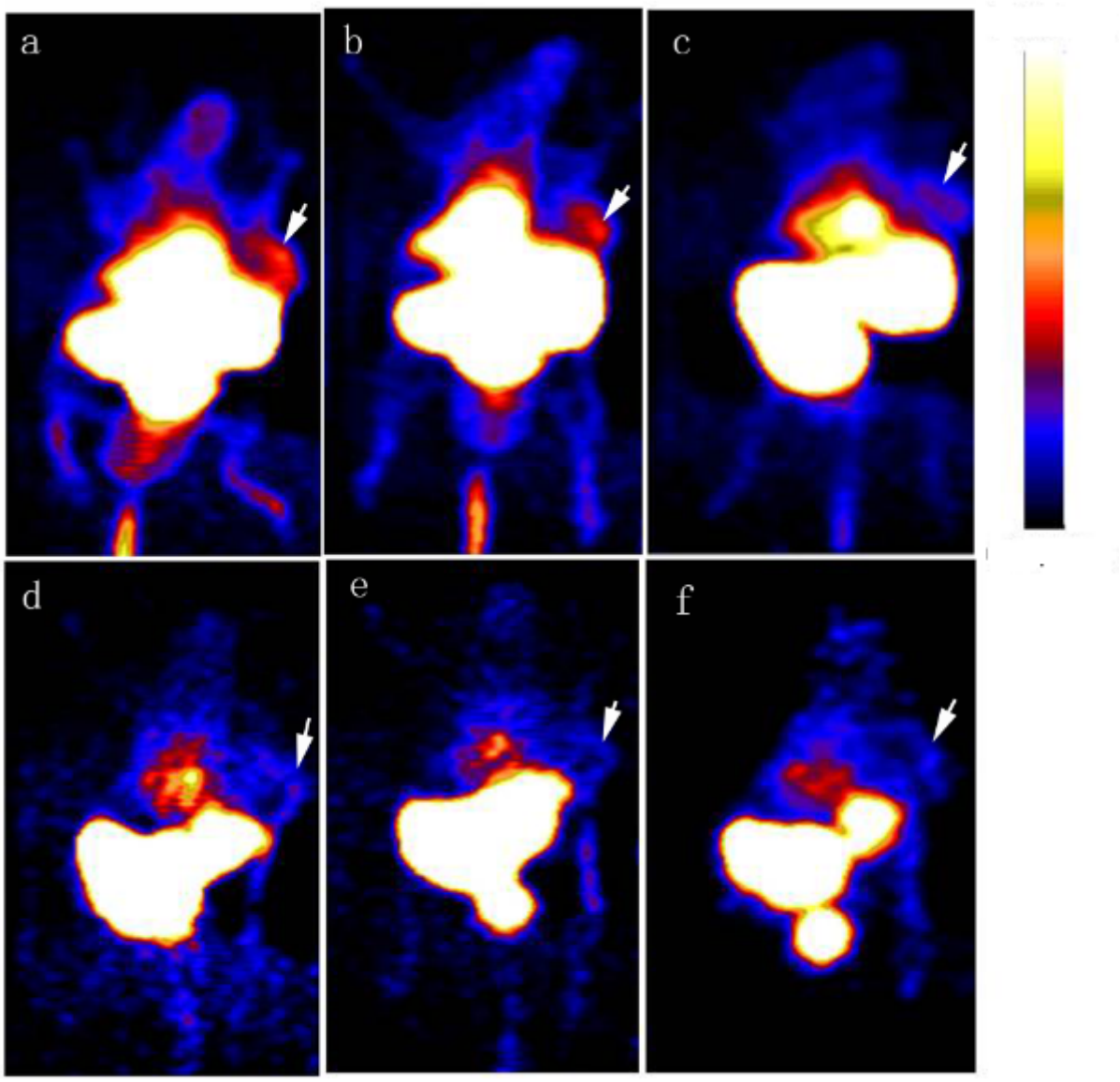


## Figure 5

Dynamic imaging of micro-PET in the MHCC-LM3 mouse model at the indicated times. A: 30 min, B: 60 min, C: 120 min, D: 240 min, E: 360 min, F: 480 min

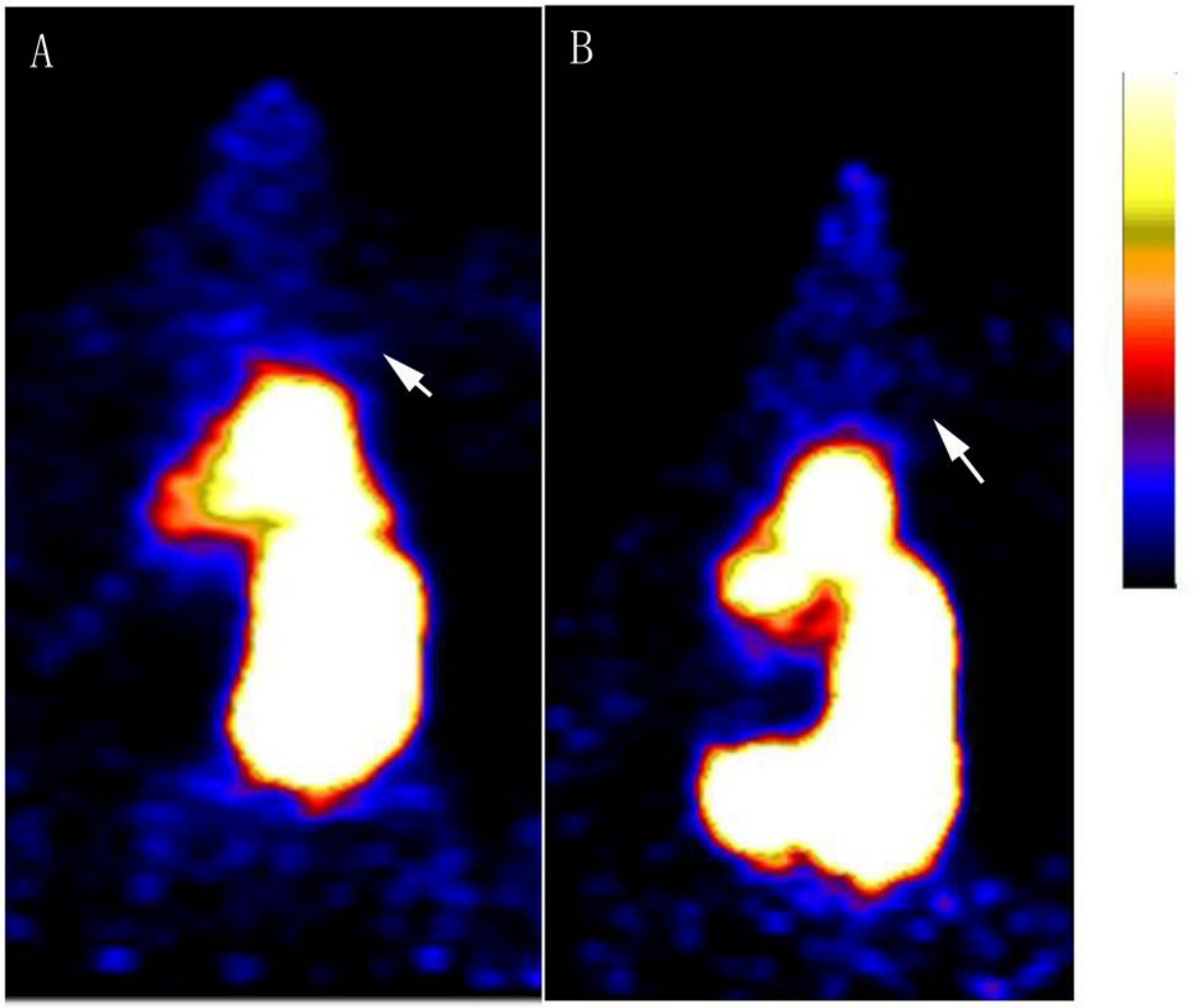


**Figure 6**

Micro-PET imaging in the MHCC-LM3 mouse model at different times in the blocked group. A: 30 min and B: 60 min.

## Supplementary Files

This is a list of supplementary files associated with this preprint. Click to download.

- senseMassspectrometry.jpg
- antisenseMassspectrometry.gif
- NC3RsARRIVEGuidelines2013.pdf